https://doi.org/10.1016/j.conbuildmat.2020.121340

Evaluation of Polyurethane Dense Graded Concrete Prepared Using the Vacuum Assisted Resin Transfer Molding Technology

Bin Hong[1], Guoyang Lu[2,3], Junling Gao[1] and Dawei Wang[1,3,*]

[1] *School of Transportation Science and Engineering, Harbin Institute of Technology, Harbin 150090, P.R. China*

binhong@hit.edu.cn (B.H.); 18S132071@stu.hit.edu.cn (J.G.)

[2] *Department of Civil and Environmental Engineering, The Hong Kong Polytechnic University, 11 Yuk Choi Road, Hung Hom, Kowloon, Hong Kong*

guoyang.lu@polyu.edu.hk (G.L.)

[3] *Institute of Highway Engineering, RWTH Aachen University, Aachen 52074, Germany*

* Corresponding author.

Postal address: 73 Huanghe Road, Nangang District, Harbin 150090, P.R. China.

Email address: wang@isac.rwth-aachen.de

Tel.: +86-451-86282840

Fax: +86-451-86282116

Abstract: In recent years, the polyurethane (PU) was widely investigated and applied in pavement engineering as a sustainable binder to facilitate pavement material with superior mechanical and functional properties. However, with higher mechanical performance, the two-component PU binders can hardly possess a gel time of more than 2 hours at room temperature, resulting in difficultly controlling the material workability through paving and compaction. Hence, the precast method concept was proposed to obtain good workability as well as the optimal engineering performances of the polyurethane mixtures (PUMs) used in pavement. In the current study, a method based on the vacuum assisted resin transfer molding (VARTM) technology was developed for the precast PUMs. The results showed that the optimal VARTM-based preparation method is to perfusion the normally compacted specimens with 2~4 wt.% PU content to obtain the optimal compaction uniformity and mechanical properties. Based on the developed methods, VARTM-formed PUM specimens were evaluated for the critical road performances, including the mechanical properties and water stability in terms of immersion Marshall stability test and freeze-thaw splitting test. By comparing the results with PUMs using the conventional compaction method, the VARTM-formed PUM shows a significant increase in both mechanical properties and water stability. Given the above excellent performances, the VARTM-formed PUMs were validated to serve as the rapid repair pavement materials or pavement materials with high waterproof performance requirements, for example, the bridge deck paving materials. This research has made a breakthrough in the construction technology of PUMs to a large extent. It has made significant contributions to the further application and promotion of PU binder in transportation infrastructures.

Keywords: Polyurethane binder; Vacuum assisted resin transfer molding; Precast pavement materials; Water stability; Pavement rapid repair

1 Introduction

In recent years, the thermosetting polyurethane mixtures (PUMs) used as the pavement materials have been paid more and more attention due to their excellent mechanical properties, durability, low-energy, and environmental friendliness [1-5]. However, in contrast to the conventional asphalt pavements, the thermosetting polyurethane (PU) pavements have not yet been widely applied. Due to the rapid curing [6] and reaction easily with water molecules [7] for the PU binders, it is very difficult to control the material workability during paving and compaction. Moreover, the PUMs possess a higher moisture susceptibility although their residual stability is still significantly higher than that of asphalt mixtures [8]. Therefore, both construction workability and moisture susceptibility of the thermosetting PU pavements are concerns [9-11].

It is known that asphalt pavements are usually constructed through the paving and compaction process. To have enough paving time, the PU binder should better have a gel time of at least 2 hours at room temperature even if the PUMs are mixed on-site. However, it is difficult for the two-component PU binders to possess high performances with a gel time of more than 2 hours at room temperature [12]. Therefore, for the two-component PU pavements, three feasible construction methods can be concluded as follows: a) develop a PU with both enough gel time and satisfactory performance; b) develop a set of equipment suitable for the construction of the PU pavements on site; c) precast the PU pavement panel in a factory. Among the three methods, the third method of precast PU pavement was investigated.

Nowadays, the precast method has already been successfully used in the cement concrete pavement [13-16] but not the asphalt pavement due to the thermoplastic nature of asphalt binder [17]. The precast method can speed up construction, reduce user delay costs and even improve the durability and performance of concrete pavement [15]. These precast concrete pavements are mainly used for the repairing, reconstruction and new construction of pavements. Moreover, the precast method can also be used to construct the prestressed concrete pavement with several clear benefits, such as reduced cracking [18], reduced slab thickness and bridging capability [14, 15], although it is very limitedly used in pavements. In addition, the precast method can be combined with intelligent monitoring technology to make smart pavement [19]. Given the excellent environmental friendly potential of the PU binder based on the life cycle analysis (LCA) [11] as well as the above advantages and application prospect of the precast method, the precast PU pavement may be able to be widely used in the future.

The traditional asphalt pavements inevitably possess voids with no less than 3% since the excessive amount of asphalt binder will cause excess oil laying on the surface of pavements. Thus, moisture can invade the asphalt pavements through the connected voids, resulting in the reduction of adhesive strength between the asphalt binders and aggregates, which further leads to the decrease of water stability of pavements [20]. However, the PU pavements cannot have excess PU on the surface even in hot summer due to a significantly higher glass transition temperature (T_g) of the PU binders than that of the asphalt binders. Therefore, it is feasible to make PU pavement with almost no voids to obtain both higher mechanical properties and water stability. It should be noted that the two-component PU is prone to produce bubbles during its reaction, which is caused by the reaction between the isocyanate component and moisture in the air [6].

In order to avoid the decrease of water stability caused by the voids derived from the formations of bubbles, the vacuum assisted resin transfer molding (VARTM) technology [21] was proposed to produce the precast PU pavement panel with fully waterproof capability. The VARTM technology has been widely used in composite material [22-24], which can significantly improve the mechanical properties of composites by eliminating voids. Hence, the VARTM-formed PU pavements are expected to have excellent mechanical properties and water stability. Furthermore, there is no harmful gas emission [25] in the closed production process, indicating that it creates almost no ecological burden. In general, in terms of the PU pavements, the VARTM technology can solve its difficult workability issue through paving and compaction.

Based on the above, the preparation method of the PUMs based on the VARTM technology was proposed and comprehensively investigated. For this purpose, the thermosetting epoxy binder with long gel time (~12 hours) was used to study the VARTM-based preparation method of the polymer mixtures (PMs), which has enough time to carry out the preparation process. It is noted that the thermosetting epoxy binders have been widely used as the epoxy asphalt binders in pavement engineering [26-28]. As same with the thermosetting PU binder, the thermosetting epoxy binder [29, 30] also faces the workability issue through paving and compaction, which can be solved by the VARTM technology. To sum up, the VARTM-based preparation method for the PMs was optimized firstly to obtain the best compaction uniformity and mechanical properties by using the epoxy binder. Subsequently, the air voids and PU content of the VARTM-formed PUMs were tested and evaluated accurately. Finally, the mechanical properties and water stability of the VARTM-formed PUMs were systematically evaluated by the immersion Marshall stability test and freeze-thaw splitting test.

2 Experimental materials and methods

2.1 Raw materials and sample preparation

2.1.1 Polymer binders

In this article, two polymers, the thermosetting polyurethane (PU) and epoxy resin were used as the binders of polymer mixtures (PMs). The epoxy resin binders were utilized to just study the preparation method for PMs based on VARTM due to its long gel time (approximately 12 hours). For the PU binders, two-component PU resin was used, which was purchased from BASF Polyurethane Specialities (China) Co., Ltd. The mass ratio between the polyol component and isocyanate component was 100 : 96. For the epoxy resin binders, bisphenol-A epoxy resin (E51, Nantong Xingchen Synthetic Materials Co. Ltd., Nantong, China) system was used, and its curing agent and accelerant are polyetheramine curing agent (D230, BASF, Shanghai, China) and tris(dimethylaminomethyl)phenol (DMP-30, Tianjin ZhongHeShengTai Commercial and Trading Co., Ltd., Tianjin, China), respectively. The mass ratio of E51, D230 and DMP-30 is 100 : 32 : 2. Both PU and epoxy binders are cured for 24 hours at room temperature. It is worth noting that different combinations of chemical substances in terms of both PU and epoxy could generate binders with different performance, for example, slow or fast curing characteristics, low or high strength, modulus and toughness. Therefore, the currently studied slow curing epoxy and PU binder do not represent all the thermosetting binders that are available for paving applications.

2.1.2 Aggregates

Basalt coarse and fine aggregates were used as the aggregates of PMs. Asphalt concrete (AC) with the maximum sieve size of 13.2 mm (AC-10, seeing in Table 1) was chosen as the aggregate gradation of PMs according to JTG F40-2004 (Technical Specification for Construction of Highway Asphalt Pavements) of China. In this article, epoxy concrete and PU concrete are called EC and PUC, respectively.

Table 1 Mass percentage (%) passing the sieve size (mm) of AC-10

Type	Sieve size (mm)								
	13.2	9.5	4.75	2.36	1.18	0.6	0.3	0.15	0.075
AC-10	100	95	60	44	32	22.5	16	11	6

2.1.3 Preparation method for PMs based on VARTM

PMs were prepared by the vacuum assisted resin transfer molding (VARTM) technology, seeing in Fig. 1. Three preparation methods were studied and compared to each other, which are classified according to the pre-treatment methods of samples. The pre-treatment methods of samples are dry mixing (DM), wet mixing (WM), preformed specimen (PS), respectively.

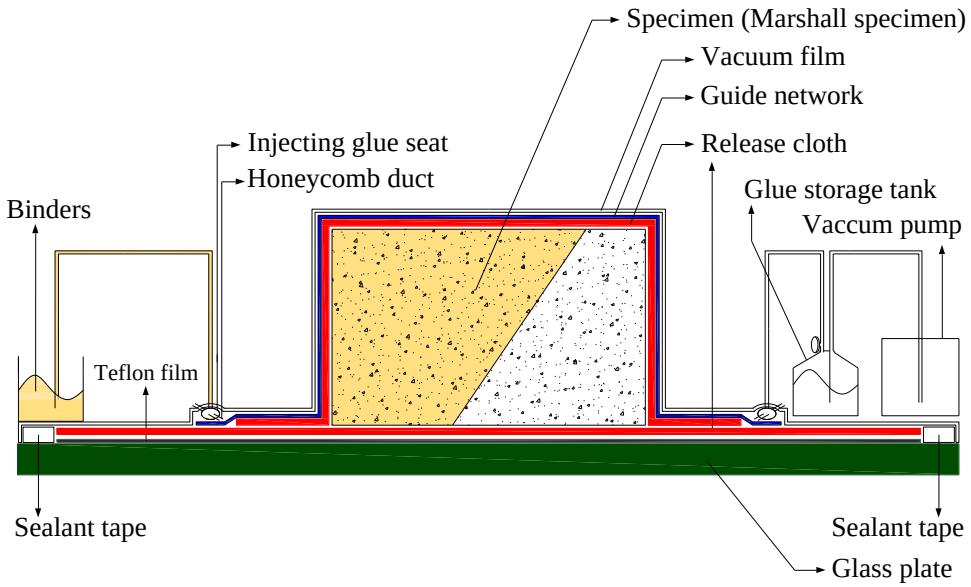

(a)

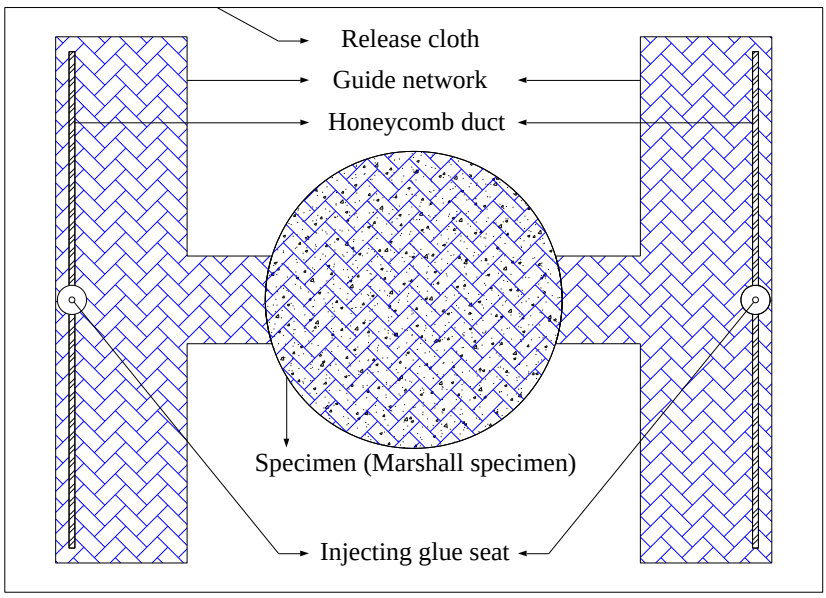

(b)

Fig. 1 The schematic diagram of the vacuum assisted resin transfer molding (VARTM) technology. (a) Front view, (b) Planform

For the DM method, the dry aggregates of different particle sizes, including mineral powder, were mixed without the polymer binders according to Table 1. For the WM method, the dry aggregates with mineral powder were mixed with 3.0 wt.% of polymer binders. For the PS method, the preformed PMs formed following the preparation method of AC-10 and cured for 24 hours, with 3.0 wt.% of polymer binders. For both the DM and WM methods, it is noted that a silicone rubber mould with the cavity size of 101.6 mm ± 0.2 mm diameter and 63.5 mm ± 0.2 mm height was used to fix the shape of samples, seeing in Fig. 2. As shown in Fig. 2, To better impregnate the sample wrapped in a silicone rubber mold, four honeycomb ducts were uniformly inlaid around the inner cavity of the mould. It is noted that samples of various shapes can be designed flexibly, such as Marshall specimen, rutting plate, ultra-thin friction course (UTFC), concrete beam, etc. The actual preparation diagram for the Marshall specimen is shown in Fig. 3. Three parallel specimens were performed for each condition.

As described above, the VARTM technology is a precast method, which has solved the potential workability issues, such as difficult paving and compaction due to the fast curing and reaction easily with moisture for the thermosetting PU binder [6, 7], during the on-site construction for the PU pavements [5, 31, 32] to a certain extent. In contrast to the popular PU modified asphalt pavements [33-36], the current technology has undoubtedly increased the cost. However, VARTM technology has avoided the cost of heating bitumen and further reduces energy consumption and environmental pollution [11]. In addition, the VARTM-formed PUMs are more considered for pavement repair, which has added more convenience to intelligent monitoring. Therefore, the relatively higher cost for the VARTM-formed PUMs is not a disadvantage in general.

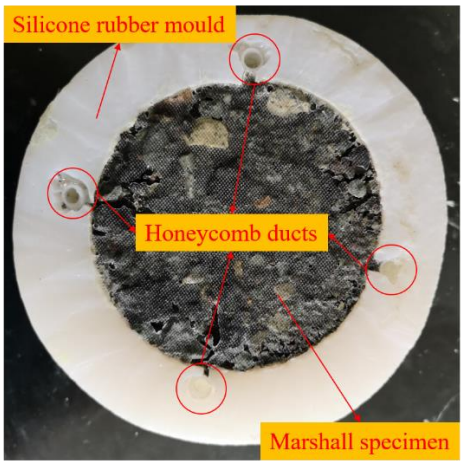

Fig. 2 Silicone rubber mould

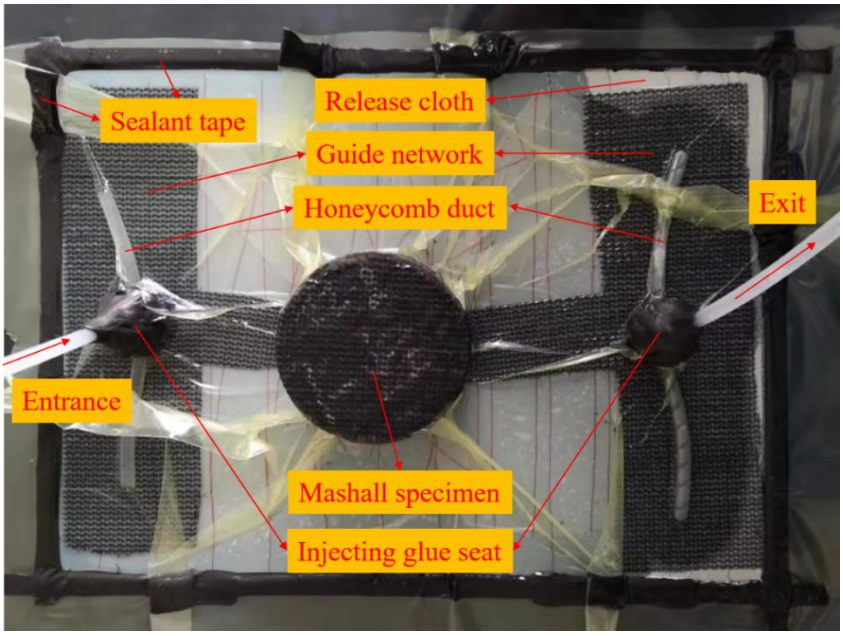

Fig. 3 The preparation diagram for the Marshall specimen

2.2 Property characterization

2.3.1 Uniformity analysis of compaction

To compare the advantages and disadvantages of the three preparation methods (DM, WM and PS), the uniformities of compaction of samples were observed and analyzed by the X-ray computed tomography (CT, Phoenix v|tome|, USA). It is worth noting that only the coarse and fine aggregates were shown in the scanned images without the polymer binders.

2.3.2 The porosity and polymer content calculation

The porosity of the preformed PMs with the polymer content of 3% was tested and calculated according to the Standard Test Methods of Bitumen and Bituminous Mixtures for Highway Engineering (JTG E20-2011, China). The polymer content (P_{b2}, %) of the VARTM-formed PMs can be calculated as follows:

$$P_{b2} = \frac{M_2 - M_1 + M_1 \times P_{b1}/100}{M_2} \times 100 \quad (1)$$

where P_{b1} is the polymer content (%) of the preformed PMs, M_1 and M_2 are the weights (g) of the preformed PMs and VARTM-formed PMs. It is noted that the calculation equation of asphalt absorption efficient (C), described in the T 0705-2011 standard from JTG E20-2011, may not be suitable for the calculation of the polymer absorption efficiency. Moreover, the PMs, like a hard stone, are very hard to break to calculate its

theoretical maximum specific gravity by the vacuum test method. Therefore, the theoretical maximum specific gravity of the PMs cannot be obtained by the above standard, which has further led to the porosity of the PMs that cannot be calculated. In this study, the CT technology [37] was utilized to calculate the porosity of the PMs.

2.3.3 Marshall stability test

According to JTG E20-2011 (T 0709-2011), the standard Marshall stability (kN) of the two PMs was tested using an universal mechanical testing machine with a range of 250 kN and a loading rate of 0.2 kN/s. Before testing, specimens were immersed in water at 60 ^{o}C for 30 min. The immersion Marshall stability was tested after water immersion at 60 ^{o}C for 30 h. Three parallel specimens were performed and the average value was calculated.

2.3.4 Freeze-thaw splitting test

According to JTG E20-2011 (T 0729-2000), the splitting strength of the two PMs before and after freeze-thawing was tested using the same universal mechanical testing machine with a range of 250 kN and a loading rate of 0.2 kN/s at 25 ^{o}C. The specimens before freeze-thawing were immersed in water at 25 ^{o}C for 2 h. After the specimens for the freeze-thaw splitting test were frozen at -18 ^{o}C for 16 h followed by immersing in water at 60 ^{o}C for 24 h and then immersed in water for 2 h at 25 ^{o}C before testing. Three parallel specimens were performed and the average value was calculated.

3 Results and discussion

3.1 Optimization of preparation method

3.1.1 Compaction uniformity analysis

The VARTM-formed samples manufactured by three pre-treatment methods, dry mixing (DM), wet mixing (WM), preformed specimen (PS), were shown in Fig. 4(a). It is noted that only the epoxy binder, due to its long gelation time (~12 h), was used to optimize the preparation method of PM based on the VARTM technology. As shown in Fig. 4(a), the aggregates of both WM and PS specimens were uniformly distributed on the surface and underside part, while the DM specimens show evident inhomogeneity of the distribution of aggregates. For the DM specimens, large particle aggregates and small particle aggregates were concentrated on the surface and underside, respectively, and potholes at the bottom were observed. Besides,

the cross-sections of both DM and WM specimens are not in a regular circle. Therefore, the DM method is not suitable for preparing the polymer mixtures (PMs).

In order to further analyze the compaction uniformity of three different pre-treatment methods, the CT images of the three specimens without voids and binders were obtained, which can be shown in Fig. 4(b)~(g). It should be noted that only one CT image of each sample was given randomly since all the CT images of the same sample are remarkably similar. As can be seen from the figure, the PS specimen has the best compaction uniformity with comparing to the other two specimens. Although the WM specimen has also a better compaction uniformity than the DM specimen, the WM specimen also has a large blank space. It can be implied that the WM method cannot guarantee a good compaction uniformity. Therefore, in terms of the compaction uniformity, the PS method gives the best performance when producing PM based on VARTM technology.

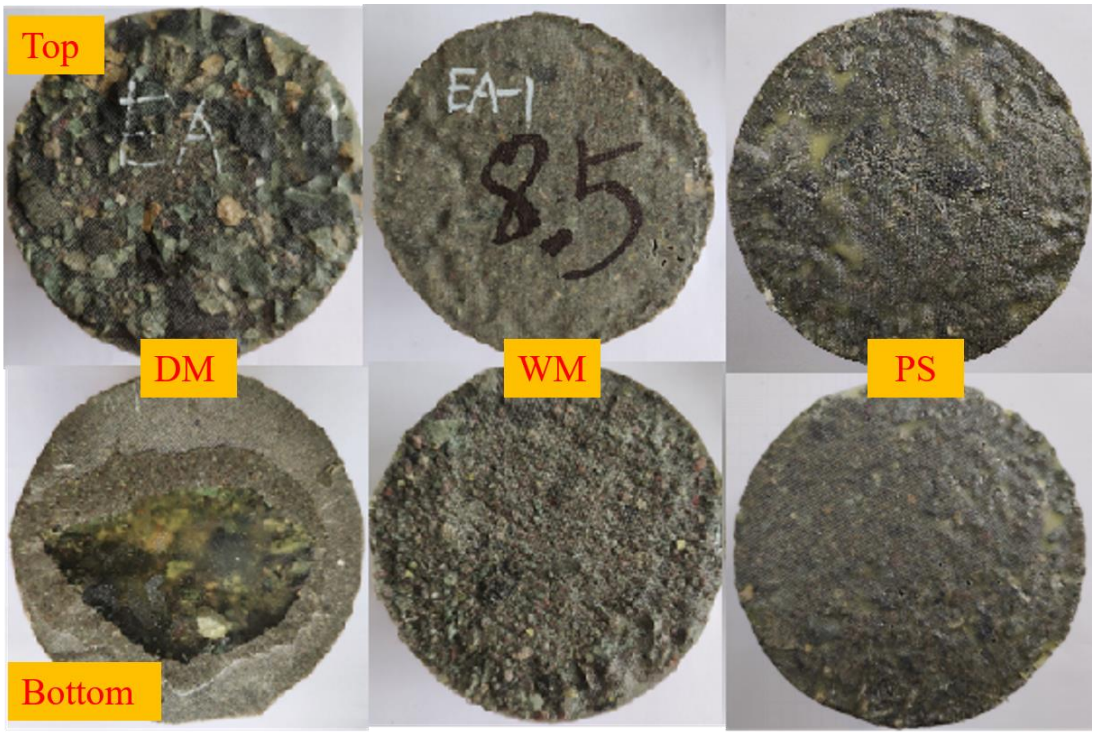

(a)

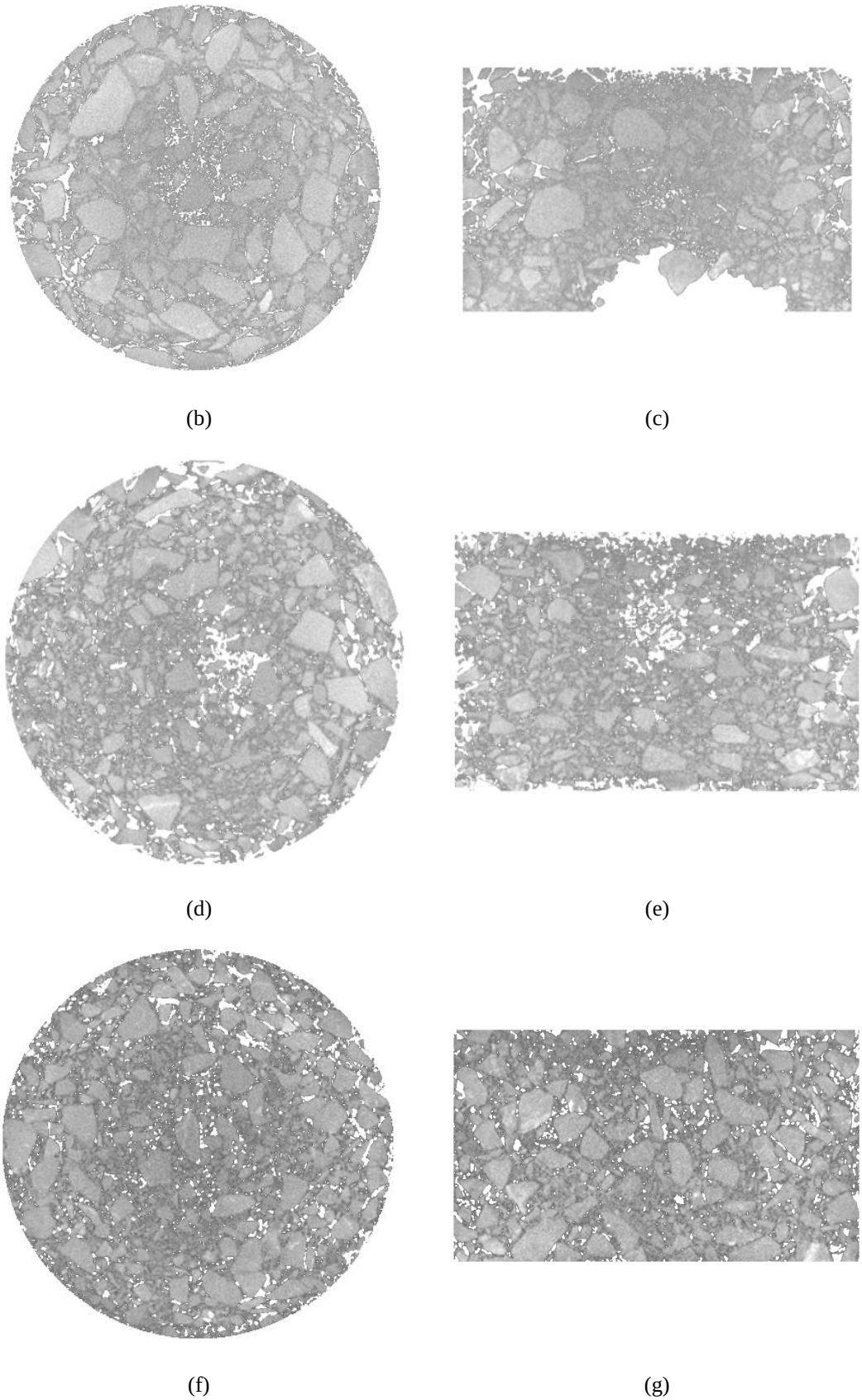

(b) (c)

(d) (e)

(f) (g)

Fig. 4 The macro and CT images of the VARTM-formed samples: (a) the top and bottom surfaces of samples manufactured by the dry mixing (DM), wet mixing (WM) and preformed specimen (PS) methods,

respectively, (b) Cross section of DM, (c) Longitudinal section of DM, (d) Cross section of WM, (e) Longitudinal section of WM, (f) Cross section of PS, (g) Longitudinal section of PS

3.1.2 Marshall stability

To further analyze the preparation methods of PMs, the Marshall stabilities of the WM and PS specimens were tested and plotted in Fig. 5. The results were also compared to the Marshall stability of epoxy mixtures (EMs) with the optimal epoxy content of 4.8% based on the former experiments. Due to the worse compaction uniformity, the Marshall stability of the DM specimen was not tested in the current section.

As can be seen in Fig. 5, the PS specimens possess the highest Marshall stability (211.5 kN ± 10.6 kN), which is significantly higher than that of both the WM and normal specimens. Although the Marshall stability of the normal specimen possesses the lowest value (149.7 kN ± 10.7 kN), its value is still visibly higher than that of AC-10 asphalt mixtures (~17.7 kN) [38]. These results show that both the WM and PS method can improve the mechanical performance of PMs due to the higher binder dosage. The superior enhancement effect can be also found pronounced by the PS method, which indicates that good compaction uniformity can significantly improve the mechanical performance of PMs. Additionally, in contrast to the traditional asphalt mixtures, the PMs possess excellent mechanical performance due to its good adhesion property between polymer and aggregates.

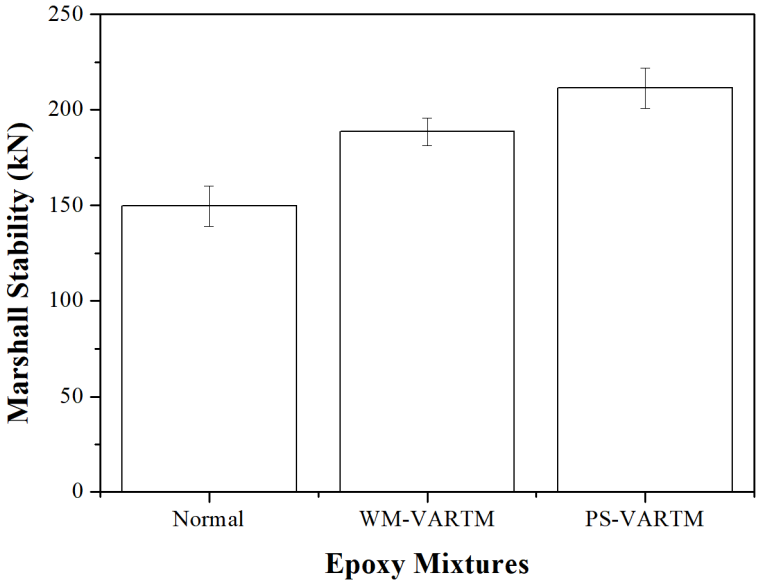

Fig. 5 Marshall stabilities of epoxy mixtures (EMs) prepared by various preparation methods

3.2 The porosity and PU content analysis

According to the optimal preparation method (the PS pre-treatment method), PUMs were prepared and shown in Fig. 6. As can be seen from figures, both the top and bottom surface of PUMs are relatively flat and smooth. The light-yellow parts shown in the figures are the PU binders. The distinct texture of the release cloth present appears on both surfaces of PUMs, which might be a way to strengthen the interfacial bond between the bottom surface of PUMs and subgrades. In terms of improving the skid resistance of PUMs, three possible methods can be adopted: a) perform grooving on the top surface like the surface treatment of concrete pavements; b) lay some dry aggregates with appropriate particle size on the top surface before the VARTM process; c) lay some impregnated aggregates with appropriate particle size on the surface of the formed PUM.

(a) (b)

Fig. 6 The VARTM-prepared PUMs according to the PS method: (a) Top surface, (b) Lower surface

The porosity of both the normal PUMs with the PU content of 4.8% and VARTM-formed PUMs was obtained by the X-ray CT technology. The scanned and treated CT images of both the normal specimen and VARTM-formed specimen are shown in Fig. 7, respectively. The black and yellow areas shown in the figures represent the voids in PUMs. According to the automatic calculation by the embedded software of CT device, the porosity of the normal specimen and VARTM-formed specimen was obtained as 5.05% and 0.40%, respectively.

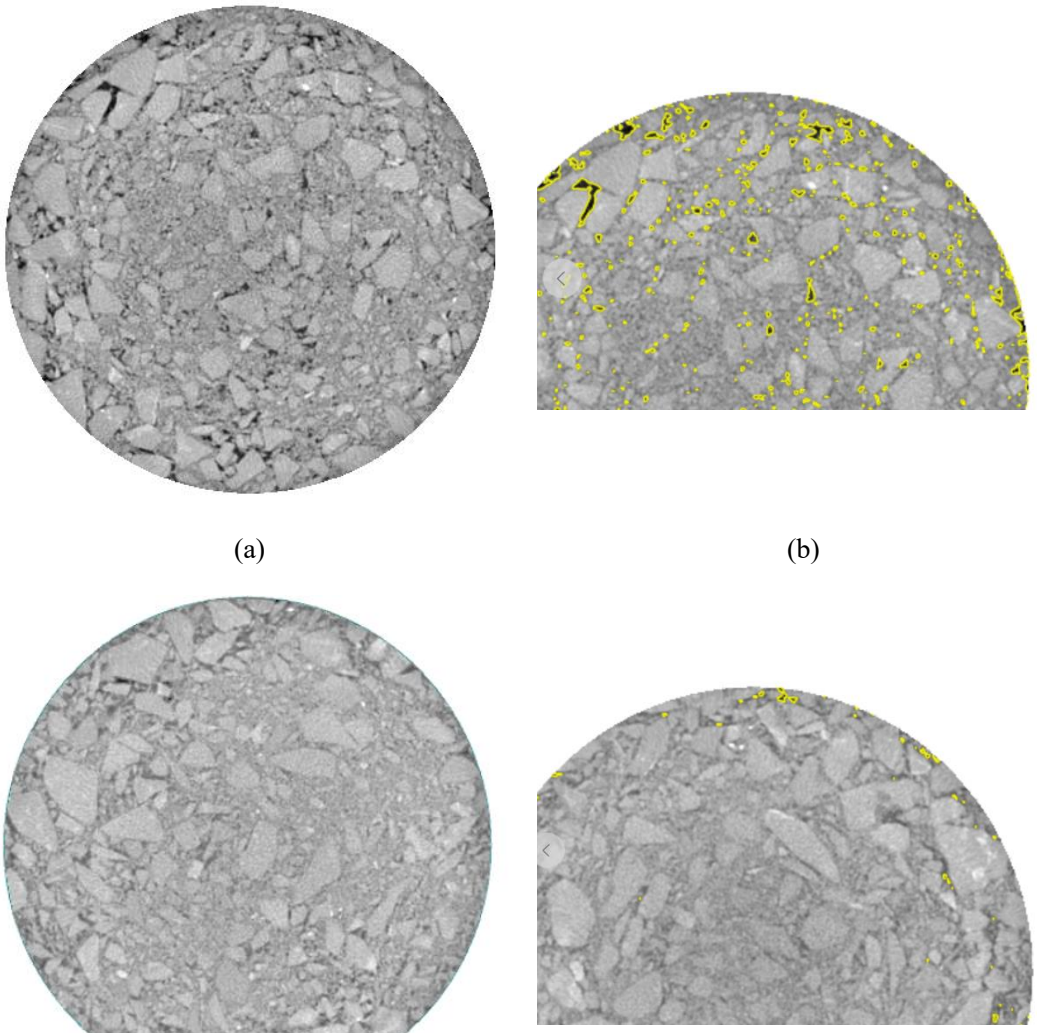

(a) (b)

(c) (d)

Fig. 7 The CT images of the normal PUM and VARTM-formed PUM: (a) Cross section of the normal PUM, (b) Void distribution of the normal PUM, (c) Cross section of the VARTM-formed PUM, (d) Void distribution of the VARTM-formed PUM

To verify the accuracy of the porosity of the VARTM-formed specimens, the weighting test in water was performed according to T 0705-2011 in JTG E20-2011. According to Eq. (1), the PU content (P_{b2}) of the VARTM-formed PUMs was equal to 11.8%. The porosity of the VARTM-formed specimens can be calculated as follows:

$$VV = \frac{V_f - (V_{sa} + V_b)}{V_f} \times 100 \quad (2)$$

where,

$$V_{\mathrm{f}} = \frac{M_{\mathrm{f}} - M_{\mathrm{w}}}{\rho_{\mathrm{w}}} \tag{3}$$

$$V_{\mathrm{sa}} = \frac{M_{\mathrm{a}}}{\rho_{\mathrm{sa}}} \tag{4}$$

$$V_{\mathrm{b}} = \frac{M_{\mathrm{b}}}{\rho_{\mathrm{b}}} \tag{5}$$

$$\rho_{sa} = \frac{100}{\frac{P_1}{\gamma_1'} + \frac{P_2}{\gamma_2'} + \cdots + \frac{P_n}{\gamma_n'}} \times \rho_{\mathrm{w}} \tag{6}$$

$$M_{\mathrm{a}} = M_2 \times \left(1 - P_{\mathrm{b}2} / 100\right) \tag{7}$$

$$M_{\mathrm{b}} = M_2 \times P_{\mathrm{b}2} / 100 \tag{8}$$

where *VV* is the porosity (%) of the VARTM-formed specimen, V_{f} is the bulk volume (cm^3) of the VARTM-formed specimen, V_{sa} is the apparent volume (cm^3) of the combined mineral aggregates including the mineral powder, V_{b} is the volume (cm^3) of the PU binder, M_{f} is the surface dry mass (g) of the VARTM-formed specimen, M_{w} is the mass (g) of the VARTM-formed specimen in water, M_{a} is the mass (g) of the mineral aggregates, M_{b} is the mass (g) of the PU binder, ρ_{w} is the density (g/cm^3) of water (equal to 0.9971 g/cm^3 at 25ºC), ρ_{sa} is the apparent density (g/cm^3) of the combined mineral aggregates, ρ_{b} is the density (g/cm^3) of the PU binder (equal to 1.20 g/cm^3), P_n is the percentage (%) of the "*n*" mineral aggregate ($P_1 + P_2 + \ldots + P_n = 100$), γ_n' is the specific gravity of the "*n*" mineral aggregate.

According to the above calculation, the porosity of the VARTM-formed specimens was equal to 0.36%, which is very close to the result (0.40%) obtained from the CT results, showing a certain reliability of the CT technology in calculating the porosity. This fairly low *VV* indicates that there are almost no voids existing in the VARTM-prepared PUMs. It can be implied that the VARTM technology can also be used in the fully waterproof pavements, such as bridge deck pavements. In addition, the VARTM technology has provided a new path for the pavement repair materials and even the smart pavement materials.

3.3 Mechanical properties and water stability

3.3.1 Mechanical properties

The Marshall stability and splitting strength of both EMs and PUMs were tested and listed in Table 3. It is worth noting that the VARTM-formed EMs were only used to study the optimal preparation method of PUMs due to the longer gel time of the epoxy system. Moreover, the Marshall stability, rather than splitting strength, was selected to evaluate different preparation methods. Therefore, the splitting strength of the VATRM-formed EMs was not given.

As can be seen in Table 3, both the Marshall stability and splitting strength of the VARTM-formed PM specimens are significantly greater than that of the normal PM specimens, indicating again that the VARTM technology can significantly improve the mechanical properties of PMs due to their high polymer binder dosage. After vacuum infusion, the polymer binders can be filled into the voids, which improves the stability of PMs.

Table 3 The Marshall stability and splitting strength of both EMs and PUMs

Mixtures	Marshall stability (kN)	Splitting strength (MPa)
Normal-EM	149.7 ± 12.7	4.19 ± 0.10
VARTM-EM[a]	188.7 ± 13.2	-
VARTM-EM[b]	211.5 ± 10.6	5.45 ± 0.15
Normal-PUM	223.1 ± 7.1	5.53 ± 0.13
VARTM-PUM[b]	298.2 ± 13.2	7.64 ± 0.15

Note: "[a]" and "[b]" mean that the specimens were prepared under the WM and PS pre-treatment methods, respectively.

In contrast to the EMs, the PUMs exhibit much more outstanding mechanical properties, which is mainly because that PU itself has higher strength, toughness and adhesive characteristics with aggregates [6]. In addition, although the normal EMs possess the lowest mechanical properties, their values are much higher than that of the conventional asphalt mixtures (AC-10) with the Marshall stability and splitting strength of ~17.7 kN [38] and no more than 1.0 MPa [39], respectively. Therefore, compared to the conventional asphalt

mixtures, the PMs possess excellent mechanical properties, especially for the PUMs, which can be applied to the projects with high mechanical performance requirements, such as the airfield pavements.

3.3.2 Immersion Marshall stability

The Marshall stabilities of both EMs and PUMs before and after water immersion were tested and plotted in Fig. 8. The VARTM-formed EM and PUM specimens were prepared under the WM and PS pre-treatment methods, respectively. As can be seen from the test result, the stability reduction of the two VARTM-formed PMs was very small after 48 hours of immersion in water, with 0.4% and 1.7% for EM and PUM, respectively. However, for the normal EM and PUM specimens, the reduction due to immersion is 6.4% and 18.4%, respectively. This is because the specimens prepared by the VARTM method had almost no voids, so water could not enter the interior of the specimens. Hence, the VARTM-formed specimens have almost no problems of moisture-induced damage.

In addition, for the conventional forming method, the reduction in the Marshall stability of the PUMs (18.4%) is significantly larger than that of the EMs (6.4%). This result shows that PUM, compared to EM, has much more remarkable Marshall stability but lower water stability under water immersion condition. It can be implied that the PU binder is overly sensitive to moisture, compared to the epoxy binder. For the two binders, the main difference between them is the core functional groups, which are -COO- and -NH-COO- for the epoxy and PU binders, respectively. When moisture invades the PUMs, strong hydrogen bonds will form between -NH- and H_2O. During this process, the intermolecular and intramolecular forces of PU will be partially destroyed [6], resulting in the degradation of the PU-aggregates adhesivity and further leading to a more severe reduction in the mechanical properties of the PUM than the EM in the early immersion. In addition, some unreacted -N=C=O- groups [6] existed in the PUMs. The above unreacted -N=C=O- groups can react with moisture and generate ureido and CO_2 [6], which further destroys the intermolecular and intramolecular forces of PU and degrades the mechanical properties of the PUM.

Nevertheless, the residual Marshall stability (~182.1 kN) of PUM after water immersion is much greater than the initial Marshall stability (~17.7 kN) of the conventional asphalt mixtures (AC-10) [38]. It might be concluded that the possible new standard for the PUMs might reduce the requirement in the loss ratio of the immersion Marshall stability.

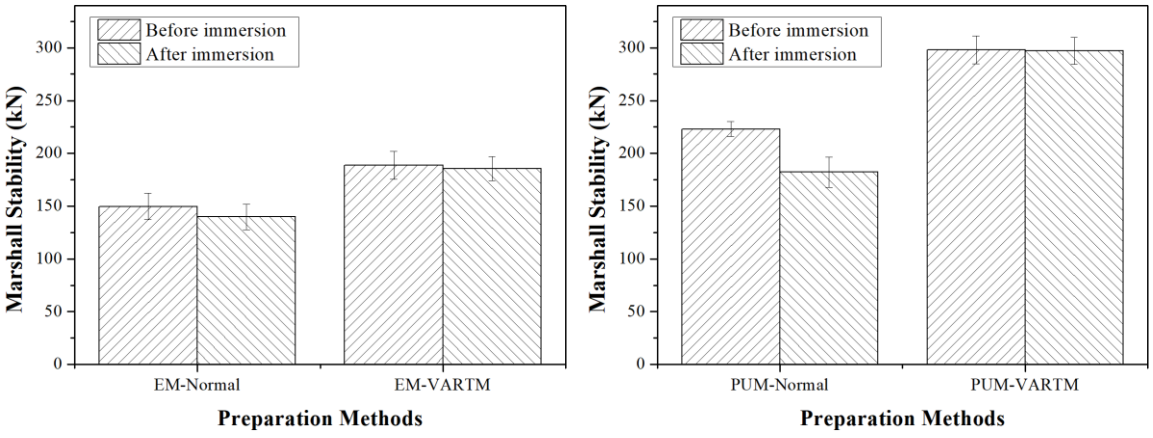

(a) (b)

Fig. 8 The Marshall stabilities of both EMs and PUMs before and after water immersion

3.3.3 Freeze-thaw splitting strength

The splitting strengths of both EMs and PUMs before and after freeze-thawing were tested and plotted in Fig. 9. It is noted that both the VARTM-formed EM and PUM specimens were prepared by the PS pre-treatment method. After freeze-thawing, the residual splitting strengths of the VARTM-formed EMs and PUMs are 99.2% and 100.4%, respectively. It is noted that the residual splitting strength of PUMs even exceeds its initial value. On the contrary, the normal EMs and PUMs have degraded the splitting strength by 6.8% and 33.4% after freeze-thawing, respectively. This result is also attributed to their near-zero porosity. Therefore, as the same with the immersion Marshall stability, it can also be considered that the VARTM-formed PMs are almost not affected by freeze-thaw.

As the same with the Marshall stability, for the conventional method, it is also abnormal that the degradation in the splitting strength of PUM (~33.4%) is worse than that of EM (~6.8%) although the former has a significantly higher splitting strength. The residual splitting strength of PUM after freeze-thawing is much less than 80% (humid region) specified in the Technical Specification for Construction of Highway Asphalt Pavements (JTG F40-2004, China), indicating that the traditional compacted PUMs have relatively weak water stability under freeze-thawing when comparing to the EMs. Fortunately, the residual splitting strength (~3.69 MPa) of PUM after freeze-thawing is much greater than the initial splitting strength (~0.75 MPa) of the traditional asphalt concrete (AC-10) [39]. It can be implied that the possible new standard for the PUMs might also reduce the requirements in the loss ratio of the freeze-thaw splitting strength.

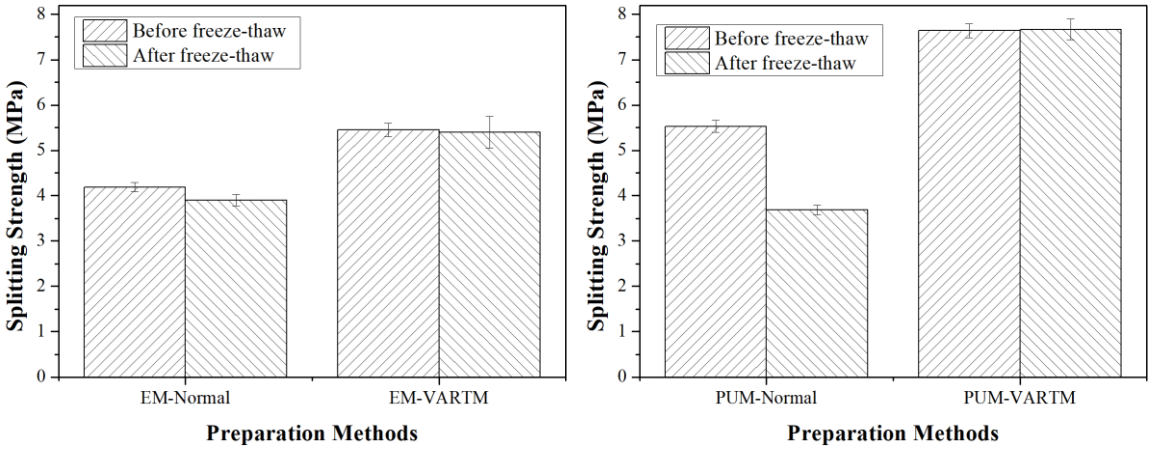

(a) (b)

Fig. 9 The splitting strength of the both EMs and PUMs before and after freeze-thawing

To visually observe the splitting failure modes of the two PMs, the splitting failure sections were shown in Fig. 10. It can be seen that, for both the EM and PUM specimens, the aggregate fractures, marked by the red circles, were found. This result has indicated that the splitting failure modes of PMs include not only the interfacial debonding but also the internal fractures of aggregates and polymer binders. It further shows that the interfacial bond strength between the aggregates and polymer binders is greater than the cohesion strength of aggregates. In addition, both the EM and PUM specimens have good perfusion effects without obvious voids and its aggregates with different particle sizes are uniformly dispersed.

(a) (b)

Fig. 10 The splitting failure section of the two PMs: (a) EM, (b) PUM

4 Conclusions

To obtain the optimal engineering performances of the PUMs used for pavement, a method based on the

VARTM technology was proposed and further optimized. Subsequently, critical road performances including the mechanical properties and water stability of VARTM-formed PUMs were characterized and compared to that of normal PUMs using the conventional compaction method. Detailed conclusions based on the present study are drawn as follows:

(1) The optimal VARTM method for preparing the PUMs mainly consists of two steps: a) the preparation of the preformed PUMs with the PU content of 2~4% using the conventional compaction method; b) the preparation of the VARTM-formed PUMs using the VARTM technology. The first step is to obtain the optimal compaction uniformity and mechanical properties.

(2) The VARTM-formed PUMs possess extremely high PU content and low percent of air void, which are approximately 11.8% and 0.36%, respectively. The PU binders are almost full of the voids of the PUMs.

(3) The VARTM technology has improved both the mechanical properties and water stability of the PUMs to the greatest extent. The VARTM-formed PUMs possess the Marshall stability and splitting strength of 298.2 kN and 7.64 MPa, respectively. In addition, the VARTM-formed PUMs are almost impervious so that water-induced distress can be completely avoided.

Given the above excellent performances, the VARTM-formed PUMs can be used as the rapid repair materials of pavements and even the pavement materials with high waterproof performance requirements, for example, the bridge deck paving materials. In addition, some smart monitoring techniques can also be incorporated into this material to realize the intelligent regional monitoring of transportation infrastructure.

Acknowledgements

This work was financially supported by the National Key Research and Development Program of China (Grant No. 2018YFB1600100), China Postdoctoral Science Foundation funded project (Grant No. BX20180088), Heilongjiang Postdoctoral Fund (Grant No. LBH-Z18083) and Key Laboratory of Road and Traffic Engineering of Ministry of Education (Grant No. K201801), Tongji University. The authors are solely responsible for the content.

References

[1] J. Chen, X.J. Yin, H. Wang, Y.M. Ding, Evaluation of durability and functional performance of porous polyurethane mixture in porous pavement, J. Clean. Prod. 188 (2018) 12-19.

[2] L. Cong, T.J. Wang, L. Tan, J.J. Yuan, J.C. Shi, Laboratory evaluation on performance of porous polyurethane mixtures and OGFC, Constr. Build. Mater. 169 (2018) 436-442.

[3] G.Y. Lu, P.F. Liu, Y.H. Wang, S. Fassbender, D.W. Wang, M. Oeser, Development of a sustainable pervious pavement material using recycled ceramic aggregate and bio-based polyurethane binder, J. Clean. Prod. 220 (2019) 1052-1060.

[4] M. Sun, Y.F. Bi, M.L. Zheng, J. Wang, L.Z. Wang, Performance of polyurethane mixtures with skeleton-interlocking structure, J. Mater. Civ. Eng. 32(2) (2020).

[5] T. Torzs, G. Lu, A.O. Monteiro, D. Wang, J. Grabe, M. Oeser, Hydraulic properties of polyurethane-bound permeable pavement materials considering unsaturated flow, Constr. Build. Mater. 212 (2019) 422-430.

[6] B. Hong, G. Xian, H. Li, Effects of water or alkali solution immersion on the water uptake and physicomechanical properties of polyurethane, Polym. Eng. Sci. 58(12) (2018) 2276-2287.

[7] B. Hong, G. Xian, Ageing of a thermosetting polyurethane and its pultruded carbon fiber plates subjected to seawater immersion, Constr. Build. Mater. 165 (2018) 514-522.

[8] T.S. Li, G.Y. Lu, D.W. Wang, B. Hong, Y.Q. Tan, M. Oeser, Key properties of high-performance polyurethane bounded pervious mixture, China. J. Highw. Transp. 32(4) (2019) 158-169.

[9] C. Leng, G.Y. Lu, J.L. Gao, P.F. Liu, X.G. Xie, D.W. Wang, Sustainable Green Pavement Using Bio-Based Polyurethane Binder in Tunnel, Materials 12(12) (2019).

[10] L. Cong, F. Yang, G.H. Guo, M.D. Ren, J.C. Shi, L. Tan, The use of polyurethane for asphalt pavement engineering applications: A state-of-the-art review, Constr. Build. Mater. 225 (2019) 1012-1025.

[11] G. Lu, Y. Wang, H. Li, D. Wang, M. Oeser, The environmental impact evaluation on the application of permeable pavement based on life cycle analysis, International Journal of Transportation Science and Technology 8(4) (2019) 351-357.

[12] C. Hepburn, Polyurethane elastomers, Springer, Netherlands, 1992.

[13] L.P. Priddy, P.G. Bly, C.J. Jackson, G.W. Flintsch, Full-scale field testing of precast Portland cement concrete panel airfield pavement repairs, Int. J. Pavement. Eng. 15(9) (2014) 840-853.

[14] A. Syed, R.S. Sonparote, Development and early-age performance of an innovative prestressed precast concrete pavement, J. Constr. Eng. M. 146(2) (2020).

[15] R. Tomek, Advantages of precast concrete in highway infrastructure construction, Procedia Engineer 196 (2017) 176-180.

[16] B. Qu, X.Z. Weng, J. Zhang, J.J. Mei, T.X. Guo, R.F. Li, S.H. An, Analysis on the deflection and load transfer capacity of a prefabricated airport prestressed concrete pavement, Constr. Build. Mater. 157 (2017) 449-458.

[17] C.M. Nwakaire, S.P. Yap, C.W. Yuen, C.C. Onn, S. Koting, A.M. Babalghaith, Laboratory study on recycled concrete aggregate based asphalt mixtures for sustainable flexible pavement surfacing, J. Clean. Prod. 262 (2020).

[18] A. Seruga, A. Smaga, R. Szydłowski, Prestressed concrete pavements, 10th International Symposium on Concrete Roads, Brussels, 2006.

[19] T. Shiraz, B. Neeraj, K. Erwin, Precast concrete pavements: Current technology and future directions, 9th International Conference on Concrete Pavements, International Society for Concrete Pavements, San Francisco, 2008.

[20] X.D. Guo, C.M. Gao, H. Wang, M.L. Zhang, The Research of Bituminous Mixture Water Stability Based on Aggregate Cleanness, Adv. Mater. Res. 255-260 (2011) 3297-3301.

[21] R. Matsuzaki, S. Kobayashi, A. Todoroki, Y. Mizutani, Flow control by progressive forecasting using numerical simulation during vacuum-assisted resin transfer molding, Compos. Part A-Appl. S. 45 (2013) 79-87.

[22] J.I. Kim, Y.T. Hwang, K.H. Choi, H.J. Kim, H.S. Kim, Prediction of the vacuum assisted resin transfer molding (VARTM) process considering the directional permeability of sheared woven fabric, Compos. Struct. 211 (2019) 236-243.

[23] M.R. Abusrea, S.W. Han, K. Arakawa, N.S. Choi, Bending strength of CFRP laminated adhesive joints fabricated by vacuum-assisted resin transfer molding, Compos. Part B-Eng. 156 (2019) 8-16.

[24] N.Q. Nguyen, M. Mehdikhani, I. Straumit, L. Gorbatikh, L. Lessard, S.V. Lomov, Micro-CT measurement of fibre misalignment: Application to carbon/epoxy laminates manufactured in autoclave and by vacuum assisted resin transfer moulding, Compos. Part A-Appl. S. 104 (2018) 14-23.

[25] M.R. Ricciardi, V. Antonucci, M. Durante, M. Giordano, L. Nele, G. Starace, A. Langella, A new cost-saving vacuum infusion process for fiber-reinforced composites: Pulsed infusion, J. Compos. Mater. 48(11) (2014) 1365-1373.

[26] Q. Lu, J. Bors, Alternate uses of epoxy asphalt on bridge decks and roadways, Constr. Build. Mater. 78 (2015) 18-25.

[27] P. Apostolidis, X.Y. Liu, S. Erkens, A. Scarpas, Use of epoxy asphalt as surfacing and tack coat material for roadway pavements, Constr. Build. Mater. 250 (2020).

[28] Q. Xiang, F.P. Xiao, Applications of epoxy materials in pavement engineering, Constr. Build. Mater. 235 (2020).

[29] P. Apostolidis, X. Liu, C. Kasbergen, M.F.C. van de Ven, G. Pipintakos, A. Scarpas, Chemo-Rheological Study of Hardening of Epoxy Modified Bituminous Binders with the Finite Element Method, Transport. Res. Rec. 2672(28) (2018) 190-199.

[30] P. Apostolidis, X. Liu, S. Erkens, A. Scarpas, Evaluation of epoxy modification in bitumen, Constr. Build. Mater. 208 (2019) 361-368.

[31] G.Y. Lu, L. Renken, T.S. Li, D.W. Wang, H. Li, M. Oeser, Experimental study on the polyurethane-bound pervious mixtures in the application of permeable pavements, Constr. Build. Mater. 202 (2019) 838-850.

[32] G.Y. Lu, P.F. Liu, T. Torzs, D.W. Wang, M. Oeser, J. Grabe, Numerical analysis for the influence of saturation on the base course of permeable pavement with a novel polyurethane binder, Constr. Build. Mater. 240 (2020).

[33] M.A. Izquierdo, F.J. Navarro, F.J. Martínez-Boza, C. Gallegos, Bituminous polyurethane foams for building applications: Influence of bitumen hardeness, Constr. Build. Mater. 30 (2012) 706-713.

[34] A.A. Cuadri, M. Garcia-Morales, F.J. Navarro, P. Partal, Isocyanate-functionalized castor oil as a novel bitumen modifier, Chem. Eng. Sci. 97 (2013) 320-327.

[35] V. Carrera, A.A. Cuadri, M. Garcia-Morales, P. Partal, Influence of the prepolymer molecular weight and free isocyanate content on the rheology of polyurethane modified bitumens, Eur. Polym. J. 57 (2014) 151-159.

[36] A.A. Cuadri, M. Garcia-Morales, F.J. Navarro, P. Partal, Processing of bitumens modified by a bio-oil-derived polyurethane, Fuel 118 (2014) 83-90.

[37] G. Xu, Y.H. Yu, D.G. Cai, G.Y. Xie, X.H. Chen, J. Yang, Multi-scale damage characterization of asphalt mixture subject to freeze-thaw cycles, Constr. Build. Mater. 240 (2020).

[38] K.B. V., K. N., The Effects of Different Binders on Mechanical Properties of Hot Mix Asphalt, International Journal of Science & Technology 2(1) (2007) 41-48.

[39] Y.Q. Bi, R. Li, S. Han, J.Z. Pei, J.P. Zhang, Development and Performance Evaluation of Cold-Patching Materials Using Waterborne Epoxy-Emulsified Asphalt Mixtures, Materials 13(5) (2020).